Soft Matter

RSC Publishing

PAPER

View Article Online
View Journal | View Issue

Cationic poly(2-oxazoline) hydrogels for reversible DNA binding

Cite this: *Soft Matter*, 2013, **9**, 4693

Matthias Hartlieb,[ab] David Pretzel,[ab] Kristian Kempe,†[ab] Carolin Fritzsche,[ab] Renzo M. Paulus,[ab] Michael Gottschaldt[ab] and Ulrich S. Schubert*[ab]

Received 11th January 2013
Accepted 8th March 2013

DOI: 10.1039/c3sm00114h

www.rsc.org/softmatter

A new 2-oxazoline monomer with a Boc-protected amino group in the side chain (BocOx) was synthesized. Homopolymerization as well as copolymerization with 2-ethyl-2-oxazoline (EtOx) revealed a pseudo first order kinetic. A series of homopolymers was synthesized, deprotected and characterized regarding their structure and thermal properties. The copolymerization with EtOx yielded a series of water soluble polymers with varying amino contents. After deprotection it was shown by the ethidium bromide assay that these polymers were able to form complexes with DNA. Treatment with epichlorohydrin leads to the formation of hydrogels. The swelling properties of the gels were investigated and it could be demonstrated that also the polymeric scaffolds were able to immobilize DNA from aqueous solution. Furthermore, the release of the DNA was accomplished using heparin.

Introduction

DNA chips and microarrays are effective tools for life science research, for instance in modern clinical diagnostics,[1] genetic analysis,[2] drug discovery,[3] and pathogen detection.[4] These efficient analytical devices are mostly characterized by a low detection level combined with a high specificity and reproducibility as well as low costs allowing high-throughput experiments.[1] The basic principle of DNA chips relies on the hybridization of target DNA molecules from the sample with specific single stranded oligonucleotides attached to a 2-dimensional solid support like glass,[5–7] silicon wafers, gold surfaces,[8] or polymers such as poly(methyl methacrylate).[9,10]

One major drawback of two-dimensional DNA chips is the limited loading capacity of surface materials and the restricted hybridization efficiency influenced by the probe density resulting in a diminished/low test signal.[11,12] To overcome these issues, a challenging alternative approach is the immobilization of single stranded DNA molecules within a 3-dimensional hydrogel matrix. Thereby, a multifold increased loading capacity compared to 2D supports can be achieved.[13,14] The high water content of the hydrogel and the resulting rapid diffusion of target DNA within the 3D matrix predestine such material attractive for DNA immobilization and hybridization. Hence, various reports describe methods for the immobilization of DNA and other biomolecules within hydrogel-like structures.[15–17]

Beside the above described detection unit of common DNA chips and microarrays, another interesting application for DNA binding hydrogels aims at a step prior to chip analysis: the isolation of DNA from the sample. It is of particular interest for fully integrated "lab on a chip" solutions that in a single device a DNA binding/purification/enrichment phase, which releases isolated DNA on a certain stimulus, can be combined with the detection area, where specific oligonucleotides are immobilized on a 3-dimensional substrate to catch and hybridize the analyte DNA.

The extraction of DNA from living or conserved tissues, cells, virus particles, or other samples is the starting point for downstream processes including diagnostic kits.[18] The general steps of nucleic acid purification include cell lysis, inactivation of cellular nucleases and separation of desired nucleic acid from cell debris.[19] Currently, there are many specialized methods for extracting DNA, which are generally divided into solution-based (*e.g.* guanidinium thiocyanate–phenol–chloroform extraction; alkaline extraction, ethidium bromide–caesium chloride gradient centrifugation) or solid phase-based methods (mostly spin columns with matrices containing silica, nitrocellulose and polyamide or anion exchange resins *e.g.* with diethylaminoethyl cellulose groups).[20–24] Whereas solid-phase nucleic acid purification systems allow quick and efficient purification compared to conventional liquid phase methods[25] and display the current state of the art, similar limitations as described for 2-dimensional DNA chip technologies occur such as limited accessible reactive surfaces. The use of functional DNA binding hydrogels for the isolation, enrichment, purification and stimuli responsive release of these biomolecules

[a]*Laboratory of Organic and Macromolecular Chemistry (IOMC), Friedrich Schiller University Jena, Humboldtstrasse 10, 07743, Jena, Germany. E-mail: ulrich.schubert@uni-jena.de*

[b]*Jena Center for Soft Matter (JCSM), Friedrich Schiller University Jena, Philosophenweg 7, 07743, Jena, Germany*

† Current address: Department of Chemical and Biomolecular Engineering, The University of Melbourne, Victoria 3010, Australia.

displays an ideal possibility to combine advantages of common liquid and solid phase extraction systems, such as a high diffusion rate, tuneable functionalities and a high reaction surface for the binding of target molecules.

For the synthesis of DNA binding hydrogels, inspiration can be found in the exploited field of non-viral gene delivery, where cationic polymers, such as poly(ethylene imine)s (PEI),[26,27] poly(L-lysin)s[28,29] and poly(methacrylate)s containing amino functionalities[30–32] have been extensively studied in the last few decades. Branched PEI (BPEI) has become the gold standard, due to its efficient polyplex formation.[33,34] The charge density and the length of the polymer backbone represent crucial factors for efficient DNA binding.[35] The synthesis path, which leads to linear PEI (LPEI), the acidic/basic hydrolysis of poly(2-oxazoline)s (POx)s in particular of poly(2-methyl-2-oxazoline) and poly(2-ethyl-2-oxazoline) (PEtOx),[36] limits the structural versatility of these gene delivery systems due to the incompatibility of most of the functional groups under these conditions. Additionally, PEI shows an unsatisfying water solubility for biological applications.[37]

Various reports have demonstrated the conjugation of PEI to other biochemically relevant polymers such as polyethylene glycol (PEG),[9–11] POxs,[38] and poly(caprolactone)[39,40] in post-polymerization reactions to overcome these issues. But also for this approach, the variety of possible end-groups for selective coupling reactions and the structural control over the PEI block are strongly limited under the hydrolysis conditions.[41]

However, the possibilities provided by the cationic ring opening polymerization (CROP) of 2-oxazolines are very versatile. It is possible to introduce functionalities into the polymer using functional initiators, end capping reagents and variation of the substituent at the 2-position of the monomer.[42–44] The living character of the reaction leads to an excellent control over the polymer length and the polydispersity index (PDI).[45] This variety is only limited by the requirements of the cationic polymerization, where nucleophiles can quench the propagating chain.

Cesana *et al.* reported the synthesis of cationic POx in 2006.[46] They used a 2-oxazoline monomer bearing a protected amino group at the 2-position to create polymers, which exhibit cationic side chains after deprotection. To the best of our knowledge, this represents the only study about cationic POxs to date. With this type of monomer it is possible to adjust the sequence, length and charge density rather easily by the CROP technique. However, the potential of this polymeric system has never been used for biochemical applications.

Moreover, (co)polymers containing amino side chains exhibit enormous potential for the design of smart hydrogels. While the synthesis of hydrogels from partially[47–49] or fully cleaved[50–52] POxs is known in the literature, the application of these systems for the reversible binding of DNA, *e.g.* for the enrichment of genes in biochip devices, has never been described to the best of our knowledge. Besides the swelling value, a basic structural requirement for such hydrogels displays the presence of amino groups in the gel matrix to interact with the DNA in solution.

This report focuses on the synthesis and detailed characterization of amino bearing POxs and their ability to bind DNA. Furthermore, hydrogels are produced on the basis of these polymers in order to act as solid substrates for the reversible binding of DNA, which is investigated using the fluorescence of ethidium bromide (EB).

Experimental part

Materials and instrumentation

All chemicals and solvents were purchased from Sigma-Aldrich, Merck, Fluka, and Acros. 2-Ethyl-2-oxazoline (EtOx) and methyl tosylate (MeTos) were distilled to dryness prior to use.

The Initiator Sixty single-mode microwave synthesizer from Biotage, equipped with a noninvasive IR sensor (accuracy: 2%), was used for polymerizations under microwave irradiation. Microwave vials were heated overnight to 110 °C and allowed to cool to room temperature under an argon atmosphere before usage. All polymerizations were carried out under temperature control.

Size-exclusion chromatography (SEC) of protected polymers was performed on a Shimadzu system equipped with a SCL-10A system controller, a LC-10AD pump, a RID-10A refractive index detector and a PSS SDV column with chloroform–triethylamine (TEA)–2-propanol (94 : 4 : 2) as eluent. The column oven was set to 50 °C. SEC of the deprotected statistical copolymers was performed on a Shimadzu system with a LC-10AD pump, a RID-10A refractive index detector, a system controller SCL-10A, a degasser DGU-14A, and a CTO-10A column oven using *N*,*N*-dimethylacetamide with 2.1 g L^{-1} LiCl as the eluent and the column oven set to 50 °C. Poly(styrene) (PS) samples were used as calibration standards for both solvent systems. SEC measurements in water were performed on a Jasco system equipped with a RI detector using a 0.1% aqueous solution of trifluoro acetic acid (TFA) with 0.05 mol L^{-1} NaCl using a pullulan standard.

Proton NMR spectroscopy (^{1}H NMR) measurements were performed at room temperature on a Bruker AC 300 and 400 MHz spectrometer, using $CDCl_3$, MeOD or DMSO-d_6 as solvents. The chemical shifts are given in ppm relative to the signal from the residual non-deuterated solvent. Fourier transform infrared (FTIR) spectroscopy was performed on an Affinity-1 FT-IR from Shimadzu, using the reflection technique. Gas chromatography (GC) was performed on a GC-2010 from Shimadzu. Acetonitrile was used as an internal standard to determine the monomer conversion.

High resolution electrospray ionization (HR-ESI) mass spectrometry (MS) was performed on a micrOTOF Q-II (Bruker Daltonics) mass spectrometer equipped with an automatic syringe pump from KD Scientific for sample injection at 4.5 kV at a desolvation temperature of 180 °C. The mass spectrometer was operating in the positive ion mode. Matrix assisted laser desorption ionization (MALDI) time of flight (ToF)-MS spectra were recorded on an Ultraflex III TOF/TOF (Bruker Daltonics GmbH, Bremen, Germany). The instrument was equipped with a frequency-tripled Nd:YAG operating at a wavelength of 355 nm. Spectra were recorded in the positive reflector and in linear mode. 2,5-Dihydroxybenzoic acid was used as a matrix for the sample preparation.

Differential scanning calorimetry (DSC) was performed on a Netzsch DSC 204 F1 Phoenix under a nitrogen atmosphere with a heating rate of 20 K min^{-1} from −100 to 200 °C. 3 Cycles were recorded for each sample. The glass transition temperature (T_g) values are reported for the second heating run. Thermo-gravimetric analysis (TGA) was performed under a nitrogen atmosphere on a Netzsch TG 209 F1 Iris in the range from room temperature to 800 °C with a heating rate of 10 K min^{-1}.

5-((*tert*-Butoxycarbonyl)amino)valeric acid[53] (2)

5-amino valeric acid (**1**, 5.15 g, 50.4 mmol) was dissolved in a mixture of aqueous sodium hydroxide solution (2 wt%, 100 mL) and dioxane (100 mL). Di-*tert*-butyldicarbonate (DiBoc) (11 g, 50.4 mmol) was dissolved in dioxane (50 mL) and added dropwise to the yellow solution. The reaction mixture was stirred for 20 h at room temperature and acidified using aqueous HCl (1 mol L^{-1}) until a pH of 3 was reached. The turbid mixture was washed with dichloromethane (3 × 50 mL), the combined organic phases were washed with water (3 × 100 mL) and dried over sodium sulfate. After evaporation of the solvent and drying in a high vacuum, the product was obtained as a white crystalline solid (8.41 g, 39 mmol, 77%).

^{1}H NMR (DMSO-d_6, 300 MHz): δ = 5.77 (0.3H, s, COOH), 4.60 (0.77H, s, NH), 3.10 (2H, s, CH_2–CH_2–N), 2.38 (2H, t, CH_2–CH_2–COO), 1.67 (2H, q, CH_2–CH_2–CH_2, 7.10 Hz), 1.54 (2H, q, CH_2–CH_2–CH_2, 6.39 Hz), 1.45 (9H, s, CH_3) ppm.

HR-ESI: *m*/*z* calc. for $C_{10}H_{19}NO_4Na$ [M + Na]: 240.1206, found: 240.1243 (error: 15.4 ppm).

FTIR: $\bar{\nu}$ (cm^{-1}) = 3374, 2983, 2951, 2879, 1720, 1683, 1520, 1486, 1462, 1444, 1431, 1415, 1388, 1361, 1330, 1277, 1242, 1204, 1165.

tert-Butyl (5-((2-chloroethyl)amino)-5-oxopentyl)carbamate (3)

To a solution of **2** (2 g, 9.21 mmol) in tetrahydrofuran (THF) (80 mL), TEA (1.276 mL, 9.21 mmol) was added and the mixture was cooled to 0 °C. After a dropwise addition of ethyl chloroformate (0.87 mL, 9.21 mmol) the reaction solution was allowed to reach room temperature and stirred for 1 h. After cooling again to 0 °C, a mixture of 2-chloroethylamine hydrochloride (1.067 g, 9.21 mmol) and TEA (1.276 mL, 9.21 mmol) in dimethylformamide (DMF) (10 mL) was added and the reaction mixture was stirred for 1.5 h.

After evaporation of the solvent, the residue was re-dissolved in dichloromethane and washed with aqueous sodium bicarbonate solution (3 × 50 mL) and brine (3 × 50 mL). The solution was dried over sodium sulfate and the solvent was evaporated. The intermediate product was obtained as a white crystalline solid (1.93 g, 6.9 mmol, 75%) and used without further purification.

^{1}H NMR ($CDCl_3$, 300 MHz): δ = 6.13 (1H, s, CH_2–NH–CO), 4.64 (1H, s, Boc–NH–CO), 3.61 (4H, m, CH_2Cl–CH_2–NH), 3.13 (2H, t, CH_2–CH_2–NHBoc, 6 Hz), 2.25 (2H, t, CH_2–CH_2–CON, 7.14 Hz), 1.68 (2H, q, CH_2–CH_2–CH_2, 7.40 Hz), 1.52 (2H, q, CH_2–CH_2–CH_2, 6.6 Hz), 1.44 (9H, s, CH_3) ppm.

HR-ESI: *m*/*z* calc. for $C_{12}H_{23}ClN_2O_4Na$ [M + Na]: 301.1289; found: 301.1318 (error: 9.6 ppm).

FTIR: $\bar{\nu}$ (cm^{-1}) = 3377, 3312, 3275, 2980, 2944, 1747, 1691, 1671, 1646, 1547, 1524, 1481, 1366, 1277, 1249, 1219, 1160.

2-(4-((*tert*-Butoxycarbonyl)amino)butyl)-2-oxazoline (BocOx) (4)

3 (1.93 g, 6.9 mmol) was dissolved in DMF (150 mL) and potassium carbonate (1.91 g, 13.8 mmol) was added. The suspension was stirred at 70 °C for 5 h. After evaporation of the solvent, the yellow oil was dissolved in dichloromethane and washed with distilled water (3 × 100 mL). The solution was dried using sodium sulfate and the solvent was evaporated under reduced pressure. The crude product was purified by distillation (6×10^{-2} mbar, 115 °C) to yield **BocOx** as a colorless viscous liquid (1 g, 4.14 mmol, 60%, ρ = 0.97 g cm^{-3}).

^{1}H NMR ($CDCl_3$, 300 MHz): δ = 4.65 (1H, s, NH), 4.21 (2H, t, CH_2–oxazoline, 9.3 Hz), 3.80 (2H, t, CH_2–oxazoline, 9.8 Hz), 3.12 (2H, t, CH_2–CH_2–NH, 6.3 Hz), 2.28 (2H, t, CH_2–CH_2–CON, 7.2 Hz), 1.65 (2H, q, CH_2–CH_2–CH_2, 7.40 Hz), 1.53 (2H, q, CH_2–CH_2–CH_2, 6.6 Hz), 1.42 (9H, s, CH_3) ppm.

HR-ESI: *m*/*z* calc. for $C_{12}H_{22}N_2O_3Na$ [M + Na]: 265.1523; found: 265.1534 (error: 4 ppm).

FTIR: $\bar{\nu}$ (cm^{-1}) = 3325, 2978, 2932, 1694, 1663, 1524, 1451, 1366, 1246, 1165.

Kinetic studies

For kinetic investigations an *in situ* oligoinitiator was synthesized from a stock solution of EtOx, MeTos (3 : 1) and acetonitrile ([M] = 1 mol L^{-1}) by microwave-assisted polymerization (140 °C, 90% conversion). Subsequently, BocOx (and EtOx for the copolymerization) was added to the initiator mixture. The stock solution was aliquoted into microwave vials (1 mL per vial) and heated in the microwave synthesizer (140 °C, varying reaction times). After polymerization, the conversions of the monomers were determined by GC with acetonitrile as an internal standard. The reaction rate constant k_P of the monomers was determined using eqn (1) and (2) assuming that the slope of the linear fit of $\ln([M]_0/[M]_t) = f(t)$ complies with k_{eff}.

$$\ln M_0 - \ln M_t = k_{eff} t \quad (1)$$

$$k_{eff} = k_p[I] \quad (2)$$

Homopolymerization of BocOx (PBocOx) (5–8)

In a microwave vial, EtOx (121 μL, 1.2 mmol), MeTos (60.6 μL, 0.4 mmol) and acetonitrile (2.95 mL) were mixed under inert conditions. After heating the vial in the microwave at 140 °C for 6 min, BocOx (403.7 μL, 4 mmol) was added under an argon stream and the mixture was heated again in the microwave synthesizer (140 °C, 5 min). The polymer solution was diluted with dichloromethane (50 mL) and extracted with saturated aqueous solution of sodium bicarbonate (3 × 50 mL) and water (3 × 50 mL). Subsequently, the solution was concentrated and the polymer was precipitated in 150 mL ice-cold diethyl ether. The white precipitate was filtered and dried in a high vacuum (392 mg, 85%).

^{1}H NMR ($CDCl_3$, 300 MHz): δ = 5.17 (s, 1H, NH), 3.44 (s, 4H, backbone), 3.10 (s, 2H, CH_2–CH_2–NH), 2.35 (s, 2H, CH_2–CH_2–CO), 1.62 (s, 2H, CH_2–CH_2–CH_2), 1.52 (s, 2H, CH_2–CH_2–CH_2), 1.41 (s, 9H, CH_3) ppm.

SEC (**5**) (eluent: $CHCl_3$–i-propanol–TEA, PS-standard): M_n = 3700 g mol^{-1}, M_w = 4700 g mol^{-1}, PDI = 1.25.

Copolymerization of EtOx and BocOx (P(EtOx-*stat*-BocOx)) (9–13)

In a microwave vial, EtOx (181.7 μL, 1.8 mmol), MeTos (90.8 μL, 0.600 mmol) and acetonitrile (11.5 mL) were mixed under inert conditions. After heating in the microwave at 140 °C for 16 min EtOx (2543 μL, 25.2 mmol) and BocOx (749 μL, 3 mmol) were added under an argon stream and the mixture was heated again in the microwave synthesizer (140 °C, 11 min). The solution was diluted with dichloromethane (100 mL) and extracted with saturated aqueous solution of sodium bicarbonate (3 × 100 mL) and water (3 × 100 mL). Subsequently, the solution was concentrated and the polymer was precipitated in 400 mL ice-cold diethyl ether. The white precipitate was filtered and dried in a high vacuum (2.77 g, 78%).

^{1}H NMR ($CDCl_3$, 300 MHz): δ = 4.99 (s, 0.2H, NH), 3.45 (s, 4H, backbone), 3.11 (s, 0.3H, CH_2–CH_2–NH (BocOx)), 2.40 (s, 1.9H, CH_2 (EtOx)), 1.92 (s, 0.3H, CH_2–CH_2–CO (BocOx)), 1.64 (s, 0.3H, CH_2–CH_2–CH_2 (BocOx)), 1.53 (s, 0.3H, CH_2–CH_2–CH2 (BocOx)), 1.42 (s, CH_3 (BocOx)), 1.21 (s, 1.3H, CH_3 (EtOx)) ppm.

SEC (**9**) (eluent: $CHCl_3$–i-propanol–TEA, PS-standard): M_n = 5300 g mol^{-1}, M_w = 5700 g mol^{-1}, PDI = 1.08.

Deprotection of PBocOx (PAmOx) (14–17)

PBocOx (**5**, 195 mg, 0.8 mmol of amino groups) was dissolved in dichloromethane (2.5 mL) and TFA (617 μL, 8 mmol) was added subsequently. After heating at 60 °C for 1 h and stirring for 24 h at room temperature, the mixture was diluted with 5 mL of methanol and precipitated in 150 mL of ice-cold diethyl ether. The yellow precipitate was re-dissolved in methanol (50 mL) and stirred with Amberlyst A21 for 24 h. Subsequently, the solution was concentrated and the polymer was precipitated in ice-cold diethyl ether (150 mL), filtered, dried in a high vacuum and obtained as a yellowish powder (103 mg, 90%).

^{1}H NMR (D_2O, 400 MHz): δ = 3.51 (s, 4H, backbone), 2.85 (s, 2H, CH_2–CH_2–NH_2), 2.42 (2H, CH_2–CH_2–CO), 1.65 (s, 4H, CH_2–CH_2–CH_2–CH_2) ppm.

SEC (**14**) (eluent: water–TFA–NaCl, pullulan-standard): M_n = 15 100 g mol^{-1}, M_w = 18 500 g mol^{-1}, PDI = 1.23.

Deprotection of P(EtOx-*stat*-BocOx) (P(EtOx-*stat*-AmOx)) (18–22)

P(EtOx-*stat*-BocOx) (**9**, 2 g) was dissolved in TFA (5 mL) and heated at 60 °C for 1 h. After stirring for 24 h at room temperature, the mixture was diluted with 10 mL methanol and precipitated in 400 mL of cold diethyl ether. The yellowish precipitate was re-dissolved in methanol (200 mL) and stirred with Amberlyst A21 for 24 h. Subsequently, the solution was concentrated and the polymer was precipitated in cold diethyl ether (400 mL), filtered, dried in a high vacuum and obtained as a yellowish powder (1.58 g, 87%).

^{1}H NMR (MeOD, 400 MHz): δ = 3.52 (s, 4H, backbone), 2.96 (0.23H, s, CH_2–CH_2–NH_2), 2.42 (2H, s, CH_2 (EtOx) + CH_2–CH_2–CO (AmOx)), 1.69 (0.41H, s, CH_2–CH_2–CH_2–CH_2 (AmOx)), 1.11 (2.8H, s, CH_3 (EtOx)) ppm.

SEC (**18**) (eluent: DMAc–LiCl, PS-standard): M_n = 8100 g mol^{-1}, M_w = 10 200 g mol^{-1}, PDI = 1.26.

Hydrogel synthesis (23–27)

P(EtOx-*stat*-AmOx) (**18**, 100 mg, 0.1 mmol NH_2-groups) was dissolved in a 5 wt% aqueous solution of sodium hydroxide. Epichlorohydrin (3.92 μL, 0.05 mmol) was added to the reaction solution and the mixture was heated at 50 °C for 1 h. Gelation occurred after 10 min. The gel was washed with methanol (5 × 20 mL) and water (2 × 20 mL) and freeze dried at −35 °C and 0.2 mbar (55 mg, 52%).

FTIR: $\bar{\nu}$ (cm^{-1}) = 2978, 2936, 1628, 1466, 1420, 1373, 1315, 1238, 1196, 1126, 1061.

Swelling studies

The water uptake of the freeze dried hydrogel samples was measured gravimetrically using centrifuge filter tubes. The filter tube was saturated with water and the excess solvent was removed by centrifugation (3000 rpm, 10 min). The tube was weighed to yield m_0. After addition of the hydrogel sample (10 to 20 mg), the tube was weighed again ($m_{0,gel}$) and the sample weight (m_{gel}) was determined using eqn (3).

$$m_{gel} = m_{0,gel} - m_0 \quad (3)$$

After swelling of the sample in water for 24 h the filter tube was centrifuged (3000 rpm, 10 min) and weighed (m_{wet}) to determine the mass of the swollen gel (m_{sw}) using eqn (4).

$$m_{sw} = m_{wet} - m_0 \quad (4)$$

The swelling degree (Q_{eq}) was calculated according to eqn (5).[54]

$$Q_{eq} = \frac{m_{sw} - m_{gel}}{m_{sw}} \times 100\% \quad (5)$$

The gelated polymer fraction (F_P) was determined using eqn (6).[54]

$$F_P = \frac{m_{th}}{m_d} \times 100\% \quad (6)$$

m_{th}: theoretical mass of the polymer in the gel (based on the mass of the polymer precursor and cross-linker), and m_d: mass of the dried sample.

Ethidium bromide assay (EBA) of P(EtOx-*stat*-PAmOx)

The complex formation of plasmid-DNA (pDNA, 4700 base pairs) with cationic polymers was detected by quenching of the EB fluorescence as described in the literature.[55]

pDNA (7.5 μg mL^{-1}) and EB (0.4 μg mL^{-1}) were dissolved in HBG-buffer (HEPES buffered glucose, pH 7) and incubated for 10 min at room temperature. 100 μL of the pDNA–EB solution were transferred to the wells of a black 96-well plate (Nunc,

Langenselbold, Germany) containing different polymer concentrations. Fluorescence was measured after 20 min of incubation with the polymer solution using a Tecan M200 Pro fluorescence microplate reader (Crailsheim, Germany) at the following wavelengths: Ex 525 nm/Em 605 nm. An internal standard containing only pDNA and EB was used to calibrate the measurements.

EBA of hydrogel samples and release studies

Between 0.8 and 2.25 mg of hydrogels per well (12-well plate) were used depending on the amino content of the samples to reach a nitrogen to phosphate (N/P) value of 1000 for every sample. The gels were swollen overnight in 250 μL of HBG-buffer (pH 7). Subsequently, 1 mL of pDNA–EB solution (containing 7.5 μg pDNA per mL and 0.4 μg EB per mL) was added and the sample aliquots of 50 μL for every time interval were taken. Fluorescence was measured in black 96-well plates using a Tecan M200 Pro fluorescence microplate reader.

For release studies, 1 mL of a mixture of heparin (6 mg mL^{-1}, 2 eq.) and EB (0.4 μg mL^{-1}) in HPG-buffer (pH 7) was added to each of the swollen gel samples. For every measuring point, 50 μL were collected and the fluorescence was determined as described above.

Microscopic detection of hydrogel supported DNA binding and release

Approximately 0.18 mg of hydrogels per well were transferred into the cavity of a clear bottom black walled 96 well plate and the gels were swollen overnight in 50 μL of HBG-buffer (pH 7). Next, 100 μL of pDNA–EB (containing 7.5 μg pDNA per mL and 0.4 μg EB per mL) solution were added and the fluorescence signal was captured directly in the wells using a fluorescence microscope (Cell Observer Z1, Carl Zeiss, Jena, Germany) equipped with a mercury arc UV lamp and the appropriate filter combinations for excitation and detection of emission. Images of a series (11 × 11 pictures per well) were captured with a 10× objective using identical instrument settings (*e.g.* UV lamp power, integration time, and camera gain) and spots of the 96 well plate were addressed using an automated XY table. Control samples contained only 100 μL of pDNA–EB (7.5 μg pDNA per mL and 0.4 μg EB per mL) and 50 μL of HBG-buffer. Microscopic detection of the resulting fluorescence signal was performed at different time points (0 min, 5 min, 30 min and 120 min).

For the release of the DNA from the hydrogel, 50 μL of heparin (60 mg mL^{-1}) were added directly to the wells and the resulting fluorescence signal was immediately analyzed microscopically as described above.

Quantification of the relative fluorescence intensity signal was performed using 8 bit, grayscale-converted images and ImageJ software. The average fluorescence intensity per pixel was obtained and the samples were normalized to the references.

Results and discussion

Monomer synthesis

The aim of this work was the synthesis of precursors for the production of hydrogels (Scheme 1), which possess the ability to reversibly bind DNA. For this purpose, (POx)s suitable for cross-linking reactions and binding of DNA are necessary. Both features can be accomplished by amino groups in the side chain of the polymers. Because free amino functionalities would quench a CROP immediately, it is necessary to use a monomer with a protected amino group, which is separated from the oxazoline ring by a spacer. The distance between the amino group and the ring should be sufficiently large to ensure that the polymerization is not influenced by the functional group. In addition, it should be short enough to yield polymers with a certain hydrophilicity.

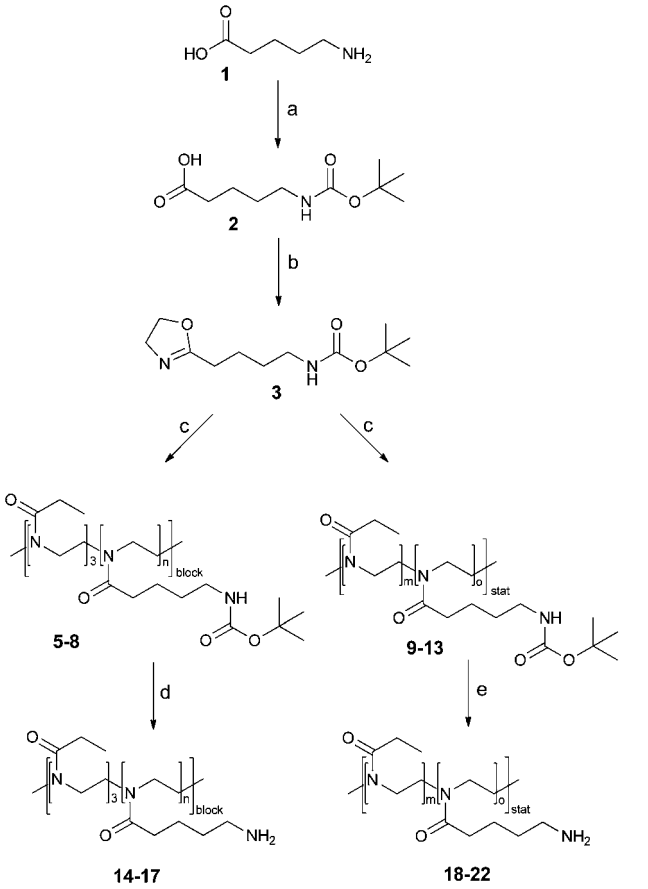

Scheme 1 Schematic overview of the synthesis of the amino bearing 2-oxazoline monomer and its polymerization with and without a comonomer. (a) diBoc, dioxane–water, NaOH; (b) (1) ethylchloroformate, chloroethylamine, TEA, DMF, (2) DMF, K_2CO_3, 60 °C; (c) μW, 140 °C, acetonitrile; (d) TFA (10 eq.), dichloromethane, 60 °C, Amberlyst A21 and (e) TFA, 60 °C, Amberlyst A21.

To this end, 5-amino valeric acid was chosen as a raw material for the monomer synthesis. The butoxy-carbonyl (Boc)-protection of the amino functionality was carried out according to a patent from Fino *et al.*[53] The amidation with chloroethylamine hydrochloride was performed in a similar fashion as reported by Cesana *et al.*[46] in a THF–DMF solvent mixture with ethyl chloroformate as an activation agent. The ^{1}H NMR spectrum of the intermediate shows that 10% of the final monomer had already been formed as indicated by the appearance of the respective oxazoline ring signals. Eventually, BocOx was obtained by treatment of the intermediate mixture with potassium carbonate in DMF. The monomer was distilled to yield a product with a purity that fulfills the requirements of CROP.

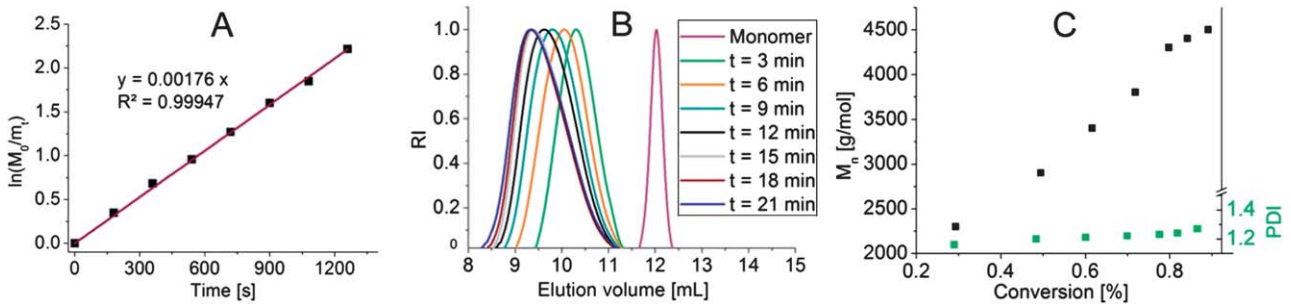

Fig. 1 Kinetic study of the homopolymerization of BocOx. (A) First-order kinetic plot, (B) SEC traces of the kinetic samples and (C) M_n against conversion plot as well as PDI values of PBocOx kinetic samples.

Cesana *et al.* reported that an initiation using small cations such as the methyl cation of the common initiators, MeTos and methyl triflate, is not suitable for this type of monomer because the cationic species will also attack the amide nitrogen of the oxazoline side chain. Preliminary tests supported these results yielding polymers with multimodal SEC traces (data not shown). Therefore, a two-step initiation was used for the polymerization of BocOx. First, the desired amount of initiator was mixed with three equivalents of EtOx in acetonitrile. This solution was heated under microwave conditions until a conversion of ~90% was reached (calculated from rate constants reported in the literature[56]). In a second step, BocOx was introduced into the microwave vial under inert conditions and polymerized in the microwave. The EtOx-oligomer produced in step one acts as an initiator for the polymerization of the BocOx monomer and the sterical hindrance of the oxazolinium species prevents an attack at the side chain. A ratio of EtOx to MeTos of 3 : 1 was necessary to ensure that all methyl cations are consumed before the addition of BocOx. Tests with a ratio of 1 : 1 resulted in significantly higher PDI values.

Synthesis and characterization of BocOx homopolymers

The first step to well-defined polymers by CROP is the knowledge about the reaction kinetic of the polymerization under the given conditions. Consequently, a kinetic study of the homopolymerization of BocOx was performed using the initiation method described above. The conversion of the monomer was determined by GC using the polymerization solvent (acetonitrile) as an internal standard. The resulting pseudo first-order kinetic plot is depicted in Fig. 1A. The linearity of the graph demonstrates a constant concentration of the propagating species during the polymerization, which is indicative of a living polymerization mechanism of BocOx. The polymerization rate was determined from the slope of the linear fit of the log plot using eqn (1) and (2). The k_p value was found to be 153 L mol^{-1} s^{-1} × 10^{-3}, which is in the same order of magnitude as EtOx in acetonitrile under the same conditions (105 L mol^{-1} s^{-1} × 10^{-3}).[56] The livingness of this polymerization is supported by the linear increase of the molar mass with conversion (Fig. 1C), as well as monomodal SEC curves and low PDI values (1.2 < PDI < 1.3) (Fig. 1B and 1C).

To investigate the properties of this polymer, four homopolymers with different lengths were synthesized using the data obtained from the kinetic study (Table 1). The values for the degree of polymerization (DP) of PBocOxs were determined by ^{1}H NMR, comparing the signal of the polymer backbone with the peaks of the initiator (tosylate) before purification. After extraction and precipitation SEC measurements revealed high PDI values for DP > 35 and, therefore, a loss of control for higher DP values. Similar observations were made for PEtOx as well, however, at higher molar masses.[57] MALDI-ToF analysis of the polymers revealed complex spectra, which is attributed to the initiation method and the resulting formation of copolymer like systems. Surprisingly, the main distribution of the spectrum of **5** is an H-initiated PBocOx without an EtOx unit as a starting group. The thermal behavior of these polymers was investigated *via* DSC and TGA (Table 1). The T_g values of PBocOxs range between 36 and 47 °C with a dependence on the molar mass. It is known that the T_g is increasing with increasing molar mass until a plateau is reached.[58] For the present polymers, the rather small change of 1 °C from DP = 35 to DP = 125 indicated that the value of 47 °C is close to the maximum T_g for this polymer class. The thermal degradation of PBocOx was investigated by TGA under a nitrogen atmosphere. The decomposition was defined as the temperature where 5 wt% of the substance is destroyed. The difference between the degradation temperatures of the samples is most likely attributed to the uncertainty of the measurement. The differing amount of EtOx cannot be

Table 1 Detailed characterization data for PBocOx and PAmOx. The M_n values were calculated from the *M*/*I* values of the polymerization

Sample number	Polymer	M_n (calc.) [g mol^{-1}]	M_n (SEC) [g mol^{-1}]	PDI	Yield [%]	T_g [°C]	Thermal stability [°C]
5	$PBocOx_{10}$	2000	2600	1.18	82	36	179
6	$PBocOx_{25}$	5600	3700	1.25	85	40	206
7	$PBocOx_{35}$	8000	6400	1.25	62	46	212
8	$PBocOx_{125}$	30 000	10 000	1.51	77	47	209
14	$PAmOx_{10}$	1800	15 700	1.19	90	—	192
15	$PAmOx_{25}$	3900	21 100	1.23	96	16	197
16	$PAmOx_{35}$	5300	32 200	1.38	95	27	201
17	$PAmOx_{125}$	18 100	52 800	2.07	94	25	190

responsible for the change since PEtOx itself decomposes thermally at around 350 °C.[59] The degradation takes place in two steps. The first one is associated with a mass loss of 41 wt% at 250 °C and indicates that the protection group is cleaved thermally.

Deprotection of the BocOx homopolymers

The chemical deprotection of the synthesized polymers was carried out under acidic conditions as commonly applied in the literature.[60] The polymers were dissolved in a 1 : 1 mixture of TFA and dichloromethane under elevated temperatures (60 °C) to yield the respective deprotected polymers (PAmOx). The resulting TFA-anion was removed with Amberlyst A21, because PAmOx is too hydroscopic for an extraction with aqueous sodium bicarbonate solution as usually applied for PEtOx. ^{1}H NMR spectroscopy proves the successful deprotection since the signal of the *tert*-butyl group has vanished in all cases (Fig. 2). SEC measurements of PAmOx were performed in water under acidic conditions. However, the standard for the measurements was pullulan which is due to its structural difference and the lack of cationic charges a poor comparison for these polymers. Thus, the obtained molar masses should be considered deliberately, also because the length of the polymer should not have changed significantly during deprotection. The MALDI-ToF spectra of PAmOx show even more distributions than the protected polymers. A reason could be the raised laser intensity, which was necessary to desorb and ionize the polymers, together with an attributed degradation. However, the most prominent difference between peaks of the major distributions is 142 g mol^{-1}, which is equal to the mass of AmOx. The glass transition of the polymers changed significantly after deprotection to lower values (16 to 27 °C).

The T_g of polymer **14** could not be determined because it interferes with a dip at around 0 °C, which is present in the DSC curves of all PAmOx samples. Most likely this drop-off is associated with adherent water molecules. PAmOx exhibits a high hydroscopic tendency. After some minutes under ambient conditions, the consistency of the polymers changes from a powder to a highly viscous liquid. Also TGA shows approximately 10% of water content for all polymers. The thermal stability does not change significantly in comparison to the protected samples.

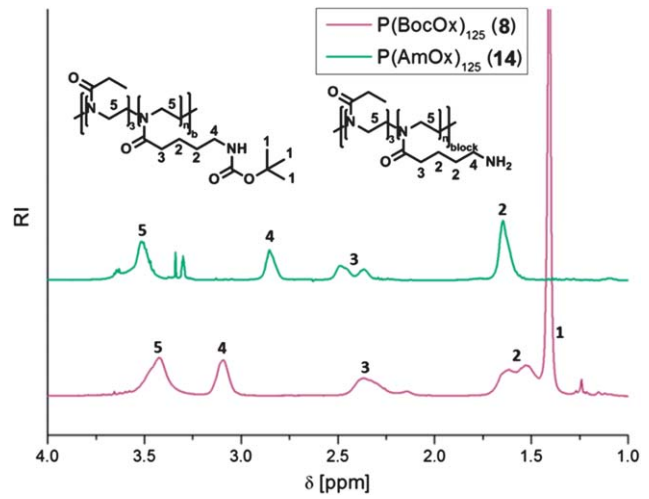

Fig. 2 Comparison of the ^{1}H NMR spectra of P(BocOx) (**8**, in $CDCl_3$, 300 MHz) and P(AmOx) (**14**, in D_2O, 400 MHz).

Statistical copolymerization

Because the water solubility of PAmOx was found to be unsatisfying, it was necessary to introduce a second monomer to yield polymers which combine functionality with hydrophilicity. The k_p value of BocOx already indicates the possibility of a statistical copolymerization with EtOx. Nevertheless, a kinetic study was performed to confirm this expectation. Using the same initiation method as described before, a stock solution of the initiating species was produced. A defined amount of BocOx and EtOx (1 : 4) was added and the solution was distributed over several microwave vials to investigate the conversions of both monomers depending on the reaction time by GC. The analytical data of the investigations are depicted in Fig. 3.

The copolymerization under microwave irradiation at 140 °C fulfills the characteristics for a living polymerization: linear pseudo first-order kinetics, a linear increase of the molar mass with conversion as well as narrow molar mass distributions. The calculated rate constants of the monomers (k_p(EtOx) = 159 (L mol^{-1} s^{-1}) × 10^{-3}, k_p (BocOx) = 175 (L mol^{-1} s^{-1}) × 10^{-3}) increased in comparison to the homo-polymerization.

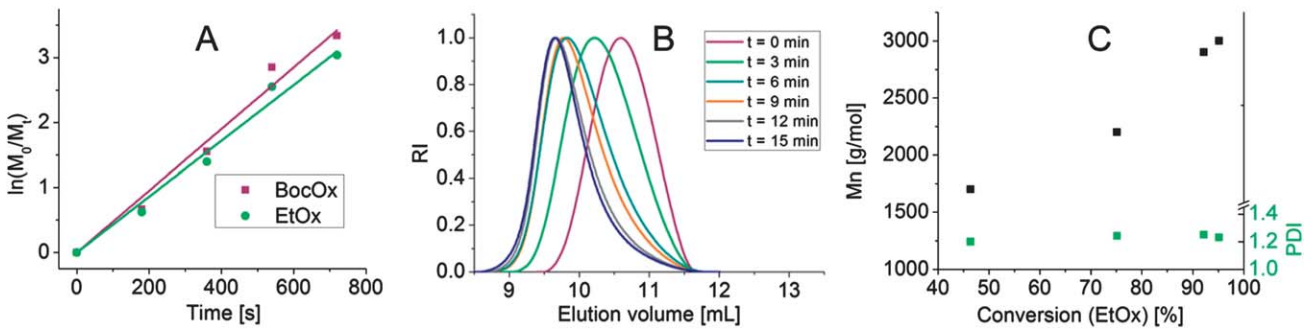

Fig. 3 Kinetic study of the statistical copolymerization of BocOx with EtOx. (A) First-order kinetic plot, (B) SEC traces of the kinetic samples and (C) M_n against conversion plot as well as PDI values of P(EtOx-*stat*-BocOx) kinetic samples.

Table 2 Detailed characterization data for P(EtOx-*stat*-BocOx) and P(EtOx-*stat*-AmOx)

Sample number	Polymer	M_n (SEC) [g mol^{-1}]	PDI	Yield [%]	BocOx/ AmOx [%]
9	P($EtOx_{43}$-*stat*-$BocOx_5$)	5400	1.08	78	10
10	P($EtOx_{39}$-*stat*-$PBocOx_7$)	5200	1.14	61	15
11	P($EtOx_{32}$-*stat*-$PBocOx_9$)	4400	1.20	75	22
12	P($EtOx_{38}$-*stat*-$PBocOx_{15}$)	4600	1.17	79	27
13	P($EtOx_{32}$-*stat*-$PBocOx_{16}$)	5400	1.17	81	33
18	P($EtOx_{43}$-*stat*-$PAmOx_5$)	8100	1.26	95	10
19	P($EtOx_{39}$-*stat*-$PAmOx_7$)	8200	1.24	90	15
20	P($EtOx_{32}$-*stat*-$PAmOx_9$)	8700	1.25	93	22
21	P($EtOx_{38}$-*stat*-$PAmOx_{15}$)	9500	1.23	89	27
22	P($EtOx_{32}$-*stat*-$PAmOx_{16}$)	9400	1.24	96	33

With this knowledge, it was possible to synthesize P(EtOx-*stat*-BocOx) with varying amounts of protected amino groups in the side chain. An overview of the produced polymers is provided in Table 2. It was aimed to synthesize P(EtOx-*stat*-BocOx) with a constant DP of 50 but varying amounts of BocOx between 10 and 30%. The DP, as well as the ratio between the monomers, was determined by ^{1}H NMR by comparison of the backbone signal with either the aromatic peaks of the tosylate or the integral of the protection group. SEC measurements reveal narrow PDI values and molar mass values in the expected range. The MALDI-ToF analysis of these polymers is rather complicated because of the broad variety of possible combinations of both monomers. However, it was possible to identify both types of repeating units in the spectra. The deprotection of the statistical copolymers was carried out in pure TFA since the reaction in a mixture of acid with dichloromethane yielded only a partial cleavage of the protection group. The TFA anion was removed in a similar fashion as for the homopolymers using Amberlyst A21. Quantitative deprotection was proven by ^{1}H NMR spectroscopy (Fig. 4).

Beside the disappearance of the *tert*-butyl peak, the signals of both middle CH_2 groups of the side chain of AmOx shift to higher ppm values and form one singlet. The SEC analysis of the copolymers was performed in DMAc (calibration against PS standard) which should enable a comparison with the protected polymers (P(EtOx-*stat*-BocOx)). However, the measured molar mass values appear to be higher in comparison to the protected polymers, which can be attributed to the positive charges of the final polymeric material. Also for the deprotected polymers, complex MALDI-ToF spectra were obtained, in which both monomer masses could be identified.

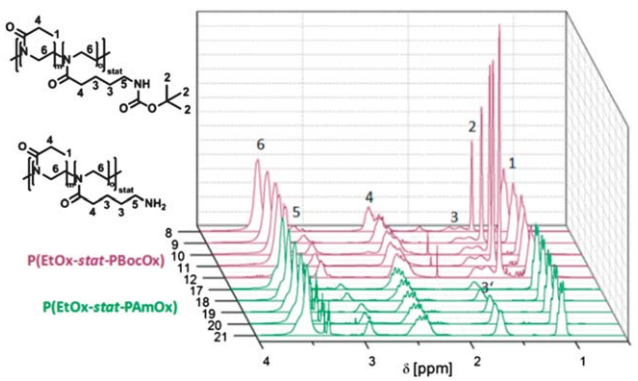

Fig. 4 Comparison of the NMR data of P(EtOx-*stat*-BocOx) (in $CDCl_3$) and the deprotected polymers P(EtOx-*stat*-AmOx) (in MeOD).

Hydrogel synthesis

To perform DNA binding and release on solid supports it was necessary to form scaffolds out of the synthesized copolymers. For this purpose, a certain amount of the amino functionalities was consumed during the reaction with a cross-linker. However, the remaining primary amines and the secondary and ternary amines which are formed during the process of linking should still possess the ability to bind negatively charged gene material.

Epichlorohydrin was chosen as a cross-linker. The epoxide functionality of the molecule reacts with amines under elevated temperature. After coupling to a polymer chain, a second epoxide function is formed under basic conditions, which can react with a second polymer chain (Scheme 2). The amount of cross-linker for the synthesis of hydrogels was chosen for every copolymer to consume only 5 amino functions per chain (Table 3). This value is sufficient to form a network while NH_2-groups are left for the DNA interaction for most of the samples. The mixture of polymer and cross-linker in a 5 wt% sodium hydroxide solution showed no gelation after 3 h at room temperature. However, heating the sample to 50 °C for 10 min resulted in the formation of a polymer network. Subsequently the gels were washed with methanol and water to extract unlinked polymer chains, residual cross-linker and to neutralize the hydrogels.

The swelling degrees were measured according to the literature by centrifugation of the swollen sample for 10 min at 3000 rpm.[54] The results are depicted in Table 3. No clear trend in the swelling degree with the ratio between the two monomers is visible, although a strong dependency on the gelated polymer fraction was observed. With an increasing amount of cross-linking, more polymer chains are incorporated into the scaffold, while the stiffness of the network increases. Therefore, an increased gelated polymer fraction indicates a more efficient cross-linking which leads to lower swelling degrees, because the balance of the Gibbs free energy of mixing and the Gibbs free energy associated with the elastic nature of the polymer network is changed.[61] However, the most outstanding property for the binding of DNA is the content of amino groups which is linearly increasing within the series of hydrogels.

DNA-binding and release

The ability of the synthesized polymers to complex DNA in aqueous solution is crucial for the aimed application. The ethidium bromide assay offers the possibility to investigate this interaction by the measurement of the fluorescence intensity of the dye. The intensity differs depending on the environment of the ethidium bromide. The dye, incorporated into a DNA helix, shows enhanced fluorescence intensity in comparison to the

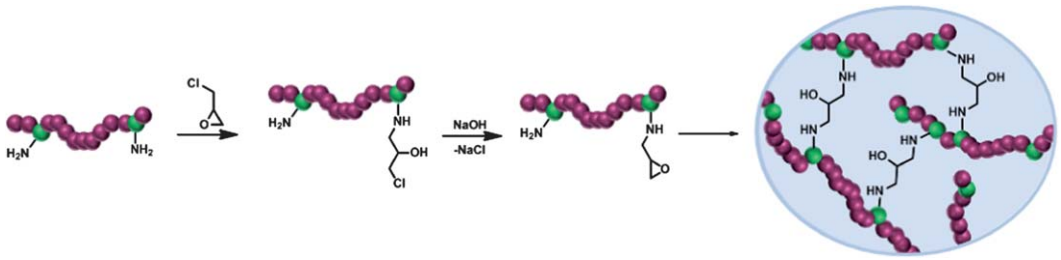

Scheme 2 Schematic representation of the hydrogel synthesis using P(EtOx-*stat*-AmOx) and epichlorohydrin.

Table 3 Overview of P(EtOx-*stat*-PAmOx) based hydrogels (per gel 100 mg of polymer were used as the starting material)

Sample number	Feed material	Epichlorohydrin [μL]	Ratio (NH_2 : ECH)	Swelling degree [%]	Gelated polymer fraction [%]
23	P($EtOx_{43}$-*stat*-$PAmOx_5$)	3.92	5 : 5	97.4 ± 0.2	34
24	P($EtOx_{39}$-*stat*-$PAmOx_7$)	3.92	7 : 5	94.6 ± 0.7	45
25	P($EtOx_{32}$-*stat*-$PAmOx_9$)	4.31	9 : 5	91.1 ± 0.3	49
26	P($EtOx_{38}$-*stat*-$PAmOx_{15}$)	3.33	15 : 5	95.7 ± 0.1	42
27	P($EtOx_{32}$-*stat*-$PAmOx_{16}$)	3.73	16 : 5	97.7 ± 0.4	32

free, dissolved species. By displacement of EB with cationic species, such as polycations, the fluorescence intensity decreases and the quality of the complexation can be determined. BPEI (10 kDa) was used as a reference for the performed tests. The results of the EBA for P(EtOx-*stat*-AmOx) are depicted in Fig. 5.

Most of the copolymers show an interaction with DNA. While a content of 10% amino bearing monomer per chain seems to be insufficient for a replacement of ethidium bromide, all other samples decrease the fluorescence intensity. Furthermore, a dependency on the strength of interaction with the amount of amino functions is clearly visible. With an increase of 5% of amino groups per chain it is possible to decrease the fluorescence intensity by around 10%. The plateau, where a further excess of positive charges is not able to replace more dye, is reached for all samples at an N/P ratio of 5. However, BPEI shows a higher complexation efficiency which can be attributed to its higher charge density. The point of saturation of BPEI is reached at an N/P ratio of 15 in this assay. To investigate the DNA binding potential of the hydrogels, the procedure for the EBA was changed. With an insoluble substrate it is not possible to dilute a stock solution and reach relatively low concentrations as performed for the copolymers. However, for comparison reasons, the chosen N/P value of 1000 was equal for all hydrogel samples in the tests. The amount of gel varied between 0.8 and 2.25 mg per well depending on the content of amines in the scaffold. Subsequently, the hydrogel samples were swollen in a 24-well plate in 250 μL of HBG buffer solution. The amount of buffer was not adjusted to the swelling degree to ensure that the dilution of DNA–EB stock solution is identical for each well.

After 24 h of swelling, 1 mL of the mentioned stock solution was added. For every time interval a sample of 50 μL was taken and investigated regarding its fluorescence intensity. The results of these measurements are depicted in Fig. 6. It is clearly visible that all gel samples decrease the fluorescence intensity

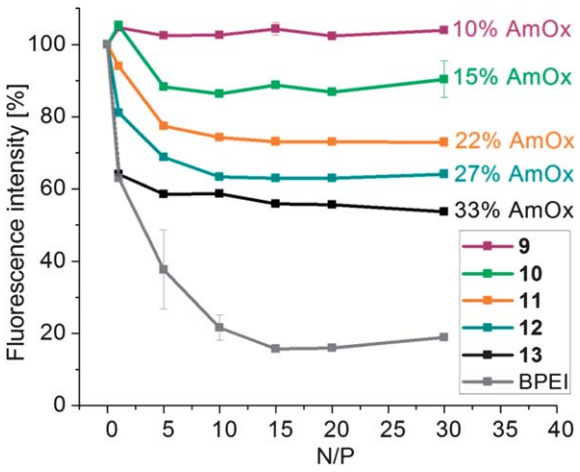

Fig. 5 EBA of P(EtOx-*stat*-AmOx) (branched polyethylene imine (BPEI) was used as positive control).

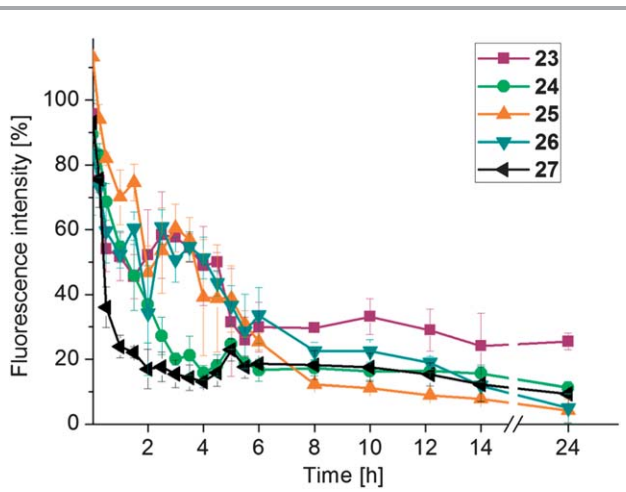

Fig. 6 EBA of P(EtOx-*stat*-AmOx) hydrogels.

over time. A solution of EB–DNA was used as a reference for each measuring point and treated in the same way as the other samples. Therefore, the decrease of intensity cannot be attributed to a degradation of the EB–DNA complex over time. In contrast to the polymeric precursors, no clear trend concerning the percental amount of amino groups is visible, though the gel with the highest content of AmOx (**27**) reaches the plateau of constant fluorescence in 2 h before the other samples. Moreover, it can be observed that the fluorescence intensity reached by the gel with the lowest amount of comonomer (**23**) is in contrast to the other samples 10% higher. A possible explanation is that this gel is saturated with DNA at the point where the plateau is reached, while the absorbance capacity of the other gel samples is high enough to bind all DNA from the solution. The residual fluorescence signal of about 10% is attributed to the remaining fluorescence of the free dye in solution. The relatively large error bars, in particular in the region of strong changes of the intensity, are attributed to the solid substrate for DNA uptake. The long adsorption period of all gels indicates a diffusion control for the process of DNA immobilization. Differences of the surface/volume ratio lead to a large deviation between the three measurements which were performed for each gel.

For biochip applications it is necessary to absorb but also to release the DNA, using a certain stimulus. For the release studies, heparin, a polyanion with multiple negative charges per repeating unit, was used to replace the DNA in the polymeric scaffold. The heparin was dissolved in an aqueous EB solution of the same concentration as applied before. The released DNA should bind to the EB in solution and increase its fluorescence. As a standard for these measurements, an EB–DNA solution was used and defined as 100%. The concentration of DNA was equal to the amount, which should be bound in the gel if all material was adsorbed during the first assay. The results of the release studies are depicted in Fig. 7. The intensity increases rapidly after the addition of heparin and reaches a plateau at *ca.* 30 min for all samples. The fluorescence value of around 60% indicates an incomplete release. But also the dilution of the test solution by the buffer, which was still present in the swollen gel sample,

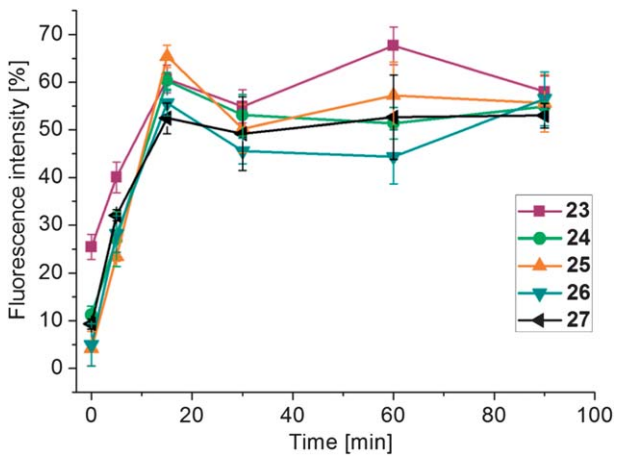

Fig. 7 Heparin induced release of DNA from P(EtOx-*stat*-AmOx) hydrogels.

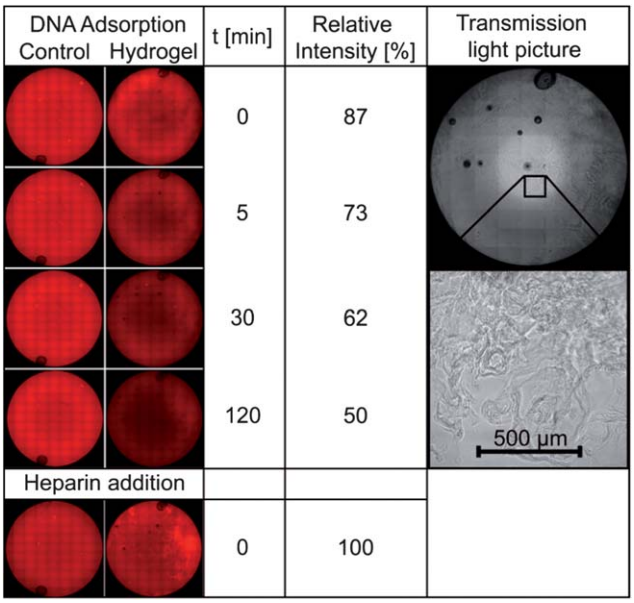

Fig. 8 Investigation of DNA binding and release using a fluorescence microscope (Gel sample **27**). Left side: absorption and release of gene material in single wells (96-well plate), indicated by fluorescence (red). Right side: transmission picture of the well with the swollen gel sample.

and a potential loss of hydrogel during the assay can be responsible for this observation.

As a final proof of the reversible absorption of DNA into P(EtOx-*stat*-AmOx) hydrogels, the process of immobilization and release was investigated using a fluorescence microscope (Fig. 8). The experiment clearly shows the decrease of fluorescence intensity of DNA–EB after the addition to the hydrogel as compared to the reference, containing a DNA–EB solution of the same concentration. The relative intensity values were calculated from the gray scale values of the samples normalized to the references. In contrast to the previous measurements, the fluorescence intensity only decreases to a value of 50%, which is related to the method. In contrast to the photometric measurements of the supernatant of P(EtOx-*stat*-AmOx) copolymers and the respective hydrogels, the microscopic study was performed with the complete sample including the hydrogel. Since the DNA, which is bound to the gel, has still free coordination sites for EB, a fluorescence signal is still detectable in the area associated with the hydrogel location. This observation was confirmed by the fact that the red fluorescence is more dominant in the boundary area of the well, where the hydrogel is mainly located, as indicated by the transmission light micrographs (Fig. 8).

The disintegration of the hydrogel-coordinated DNA turned out to be even faster than in the previous investigations. As indicated by the obtained gray scale values, a full release of DNA occurs immediately after the addition of heparin. The pictures clearly show an increased intensity in the area of the hydrogel which proves that the DNA is replaced by heparin but not diffused out of the gel (Fig. 8). This observation supports the assumption that the release of gene material from the hydrogels is diffusion controlled.

Conclusion and outlook

In summary it was shown that amino bearing POx can be synthesized starting from an oxazoline monomer with a protected amino functionality at the 2-position (BocOx). Kinetic studies were performed for a homopolymerization and a series of polymers (PBocOx) were synthesized. The deprotected polymers (PAmOx) were characterized regarding their structure, T_g values and thermal degradation behavior. Because of a lack of water solubility of the resulting homopolymers, EtOx was used as a comonomer. Kinetic investigations revealed that both monomers possess similar polymerization rates in a copolymerization. P(EtOx-*stat*-BocOx) were synthesized with differing amounts of BocOx (10 to 33%) and deprotected subsequently. It was shown that these polymers are able to form complexes with DNA using the EB-assay. The strength of the interaction correlates directly with the amount of amino groups per polymer. P(EtOx-*stat*-AmOx)s were cross-linked using epichlorohydrin to form hydrogels. These polymeric scaffolds were investigated regarding their swelling degrees and ability to absorb DNA from aqueous solution in a similar manner as investigated for the polymer precursors. It was shown that all hydrogels possess the ability to immobilize DNA from solution. It was also possible to release DNA from the scaffolds by the addition of heparin as a polyanion. Amounts larger than 60% of the initial DNA quantity could be set free again by the replacement with heparin. The process was also investigated using a fluorescence microscope, proving the previous findings and indicating quantitative release.

Further studies will focus on the release of gene material from hydrogels by a certain stimulus. While heparin is sufficient to replace the DNA in the first tests, a release induced by temperature or pH change would be more meaningful with regard to the targeted applications. Furthermore, biochips will be equipped with the produced hydrogels by inkjet printing to check their ability for DNA enrichment also on a smaller scale.

Acknowledgements

The authors would like to thank the Bundesministerium für Bildung und Forschung (Germany) for funding (project: BASIS, 03WKCB01C). Kristian Kempe acknowledges the Alexander von Humboldt foundation. Grateful thanks to Esra Altuntas (Friedrich Schiller University Jena) for ESI-MS, Sarah Crotty (Friedrich Schiller University Jena) for MALDI-ToF-MS measurements and Dr. Stephanie Schubert for correction of the manuscript.

Notes and references

1 J. Peeters and P. Van der Spek, *Cell Biochem. Biophys.*, 2005, **43**, 149–166.
2 T. R. Gingeras, D. Y. Kwoh and G. R. Davis, *Nucleic Acids Res.*, 1987, **15**, 5373–5390.
3 J. M. Anderton, R. Tokarz, C. D. Thill, C. J. Kuhlow, C. S. Brooks, D. R. Akins, L. I. Katona and J. L. Benach, *Infect. Immun.*, 2004, **72**, 2035–2044.
4 C. W. Wong, T. J. Albert, V. B. Vega, J. E. Norton, D. J. Cutler, T. A. Richmond, L. W. Stanton, E. T. Liu and L. D. Miller, *Genome Res.*, 2004, **14**, 398–405.
5 L. G. Britcher, D. C. Kehoe, J. G. Matisons, R. S. C. Smart and A. G. Swincer, *Langmuir*, 1993, **9**, 1609–1613.
6 B. Joos, H. Kuster and R. Cone, *Anal. Biochem.*, 1997, **247**, 96–101.
7 Y.-H. Rogers, P. Jiang-Baucom, Z.-J. Huang, V. Bogdanov, S. Anderson and M. T. Boyce-Jacino, *Anal. Biochem.*, 1999, **266**, 23–30.
8 A. B. Steel, R. L. Levicky, T. M. Herne and M. J. Tarlov, *Biophys. J.*, 2000, **79**, 975–981.
9 F. Fixe, M. Dufva, P. Telleman and C. B. V. Christensen, *Nucleic Acids Res.*, 2004, **32**, e9.
10 E. Waddell, Y. Wang, W. Stryjewski, S. McWhorter, A. C. Henry, D. Evans, R. L. McCarley and S. A. Soper, *Anal. Chem.*, 2000, **72**, 5907–5917.
11 A. W. Peterson, R. J. Heaton and R. M. Georgiadis, *Nucleic Acids Res.*, 2001, **29**, 5163–5168.
12 J. B. Rampal, *Microarrays: Synthesis Methods*, Humana Press, Totowa, 2001.
13 P. Anzenbacher Jr, Y.-l. Liu and M. E. Kozelkova, *Curr. Opin. Chem. Biol.*, 2010, **14**, 693–704.
14 D. Guschin, G. Yershov, A. Zaslavsky, A. Gemmell, V. Shick, D. Proudnikov, P. Arenkov and A. Mirzabekov, *Anal. Biochem.*, 1997, **250**, 203–211.
15 O. Okay, *J. Polym. Sci., Part B: Polym. Phys.*, 2011, **49**, 551–556.
16 F. Kivlehan, M. Paolucci, D. Brennan, I. Ragoussis and P. Galvin, *Anal. Biochem.*, 2012, **421**, 1–8.
17 J. Liu, *Soft Matter*, 2011, **7**, 6757–6767.
18 M. Wink, *An Introduction to Molecular Biotechnology: Molecular Fundamentals, Methods and Applications in Modern Biotechnology*, Wiley-VCH, Weinheim, Germany, 2006.
19 K. Doyle, *The Source of Discovery: Protocols and Applications Guide*, PROMEGA, Madison, Wis, USA, 1996.
20 L. Buckingham and M. L. Flaws, *Molecular Diagnostics: Fundamentals, Methods, & Clinical Applications*, F. A. Davis, Philadelphia, Pa, USA, 2007.
21 J. Sambrook and D. Russel, *Molecular Cloning: A Laboratory Manual*, Cold Spring Harbor Laboratory Press, New York, NY, USA, 2001.
22 *Pierce Strong Ion Exchange Spin Columns*, Thermo Scientific, New Hampshire, NH, USA, 2007.
23 *QIAGEN Genomic DNA Handbook*, QIAGEN, Valencia, Calif, USA, 2001.
24 D. T. Gjerse, L. Hoang and D. Hornby, *RNA Purification and Analysis: Sample Preparation, Extraction, Chromatography*, Wiley-VCH, Weinheim, Germany, 2009.
25 K.-H. Esser, W. H. Marx and T. Lisowsky, *BioTechniques*, 2005, **39**, 270–271.
26 H. Pollard, J.-S. Remy, G. Loussouarn, S. Demolombe, J.-P. Behr and D. Escande, *J. Biol. Chem.*, 1998, **273**, 7507–7511.
27 O. Boussif, F. Lezoualc'h, M. A. Zanta, M. D. Mergny, D. Scherman, B. Demeneix and J. P. Behr, *Proc. Natl. Acad. Sci. U. S. A.*, 1995, **92**, 7297–7301.

28 G. Y. Wu and C. H. Wu, *J. Biol. Chem.*, 1988, **263**, 14621–14624.
29 G. Y. Wu and C. H. Wu, *J. Biol. Chem.*, 1987, **262**, 4429–4432.
30 J. Luten, N. Akeroyd, A. Funhoff, M. C. Lok, H. Talsma and W. E. Hennink, *Bioconjugate Chem.*, 2006, **17**, 1077–1084.
31 A. M. Funhoff, C. F. van Nostrum, A. P. C. A. Janssen, M. H. A. M. Fens, D. J. A. Crommelin and W. E. Hennink, *Pharm. Res.*, 2004, **21**, 170–176.
32 P. van de Wetering, J.-Y. Cherng, H. Talsma and W. E. Hennink, *J. Controlled Release*, 1997, **49**, 59–69.
33 M. A. Mintzer and E. E. Simanek, *Chem. Rev.*, 2008, **109**, 259–302.
34 D. D. Dunlap, A. Maggi, M. R. Soria and L. Monaco, *Nucleic Acids Res.*, 1997, **25**, 3095–3101.
35 H. P. C. Van Kuringen, J. Lenoir, E. Adriaens, J. Bender, B. G. De Geest and R. Hoogenboom, *Macromol. Biosci.*, 2012, **12**, 1114–1123.
36 L. Tauhardt, K. Kempe, K. Knop, E. Altuntaş, M. Jäger, S. Schubert, D. Fischer and U. S. Schubert, *Macromol. Chem. Phys.*, 2011, **212**, 1918–1924.
37 A. Kichler, *J. Gene Med.*, 2004, **6**, 3–10.
38 G.-H. Hsiue, H.-Z. Chiang, C.-H. Wang and T.-M. Juang, *Bioconjugate Chem.*, 2006, **17**, 781–786.
39 R. Arote, T.-H. Kim, Y.-K. Kim, S.-K. Hwang, H.-L. Jiang, H.-H. Song, J.-W. Nah, M.-H. Cho and C.-S. Cho, *Biomaterials*, 2007, **28**, 735–744.
40 X. Shuai, T. Merdan, F. Unger, M. Wittmar and T. Kissel, *Macromolecules*, 2003, **36**, 5751–5759.
41 M. Jäger, S. Schubert, S. Ochrimenko, D. Fischer and U. S. Schubert, *Chem. Soc. Rev.*, 2012, **41**, 4755–4767.
42 B. Guillerm, S. Monge, V. Lapinte and J.-J. Robin, *Macromol. Rapid Commun.*, 2012, **33**, 6000–6016.
43 K. Kempe, R. Hoogenboom, M. Jaeger and U. S. Schubert, *Macromolecules*, 2011, **44**, 6424–6432.
44 K. Kempe, M. Lobert, R. Hoogenboom and U. S. Schubert, *J. Polym. Sci., Part A: Polym. Chem.*, 2009, **47**, 3829–3838.
45 N. Adams and U. S. Schubert, *Adv. Drug Delivery Rev.*, 2007, **59**, 1504–1520.
46 S. Cesana, J. Auernheimer, R. Jordan, H. Kessler and O. Nuyken, *Macromol. Chem. Phys.*, 2006, **207**, 183–192.
47 Y. Chujo, Y. Yoshifuji, K. Sada and T. Saegusa, *Macromolecules*, 1989, **22**, 1074–1077.
48 Y. Chujo, K. Sada and T. Saegusa, *Macromolecules*, 1990, **23**, 2636–2641.
49 Y. Chujo, K. Sada and T. Saegusa, *Polym. J.*, 1993, **25**, 599–608.
50 J.-J. Yuan and R.-H. Jin, *Langmuir*, 2005, **21**, 3136–3145.
51 D. Kim and K. Park, *Polymer*, 2004, **45**, 189–196.
52 F. Khan, R. S. Tare, R. O. C. Oreffo and M. Bradley, *Angew. Chem., Int. Ed.*, 2009, **48**, 978–982.
53 Fino, *et al.*, *US Pat.*, US 4476229, 1984.
54 A. Koschella, M. Hartlieb and T. Heinze, *Carbohydr. Polym.*, 2011, **86**, 154–161.
55 A. N. Zelikin, E. S. Trukhanova, D. Putnam, V. A. Izumrudov and A. A. Litmanovich, *J. Am. Chem. Soc.*, 2003, **125**, 13693–13699.
56 R. Hoogenboom, M. W. M. Fijten, H. M. L. Thijs, B. M. van Lankvelt and U. S. Schubert, *Des. Monomers Polym.*, 2005, **8**, 659–671.
57 F. Wiesbrock, R. Hoogenboom, M. A. M. Leenen, M. A. R. Meier and U. S. Schubert, *Macromolecules*, 2005, **38**, 5025–5034.
58 P. Claudy, J. M. Létoffé, Y. Camberlain and J. P. Pascault, *Polym. Bull.*, 1983, **9**, 208–215.
59 C. Weber, A. Krieg, R. M. Paulus, H. M. L. Lambermont-Thijs, C. R. Becer, R. Hoogenboom and U. S. Schubert, *Macromol. Symp.*, 2011, **308**, 17–24.
60 P. G. M. Wuts and T. W. Greene, *Greene's Protective Groups in Organic Synthesis*, Wiley-VCH, Weinheim, 4th edn, 2006.
61 M. E. Byrne, K. Park and N. A. Peppas, *Adv. Drug Delivery Rev.*, 2002, **54**, 149–161.

